Title

X-ray-induced acoustic computed tomography for guiding prone stereotactic partial breast irradiation: a simulation study

Journal

Medical Physics, 47(9)

ISSN

0094-2405

Authors

Zheng, Yue
Samant, Pratik
Merill, Jack
et al.

Publication Date

2020-09-01

DOI

10.1002/mp.14245

Peer reviewed

HHS Public Access

Author manuscript

Med Phys. Author manuscript; available in PMC 2020 December 09.

Published in final edited form as:

Med Phys. 2020 September ; 47(9): 4386–4395. doi:10.1002/mp.14245.

X-ray-induced acoustic computed tomography for guiding prone stereotactic partial breast irradiation: a simulation study

Yue Zheng,
Shandong Key Laboratory of Medical Physics and Image Processing & Shandong Provincial Engineering and Technical Center of Light Manipulations, School of Physics and Electronics, Shandong Normal University, Jinan 250358, China; School of Electrical and Computer Engineering, University of Oklahoma, Norman, OK 73019, USA

Pratik Samant,
School of Biomedical Engineering, University of Oklahoma, Norman, OK 73019, USA

Jack Merill,
School of Electrical and Computer Engineering, University of Oklahoma, Norman, OK 73019, USA

Yong Chen,
Department of Radiation Oncology, University of Oklahoma Health Sciences Center, Oklahoma City, OK 73104, USA

Salahuddin Ahmad,
Department of Radiation Oncology, University of Oklahoma Health Sciences Center, Oklahoma City, OK 73104, USA

Dengwang Li[a)],
Shandong Key Laboratory of Medical Physics and Image Processing & Shandong Provincial Engineering and Technical Center of Light Manipulations, School of Physics and Electronics, Shandong Normal University, Jinan 250358, China

Liangzhong Xiang[a)]
School of Electrical and Computer Engineering, University of Oklahoma, Norman, OK 73019, USA

Abstract

Purpose: The aim of this study is to investigate the feasibility of x-ray-induced acoustic computed tomography (XACT) as an image guidance tool for tracking x-ray beam location and monitoring radiation dose delivered to the patient during stereotactic partial breast irradiation (SPBI).

Methods: An in-house simulation workflow was developed to assess the ability of XACT to act as an *in vivo* dosimetry tool for SPBI. To evaluate this simulation workflow, a three-dimensional (3D) digital breast phantom was created by a series of two-dimensional (2D) breast CT slices from

[a)]Authors to whom correspondence should be addressed. dengwang.li@139.com; xianglzh@ou.edu. Telephones: 159-319-1585; 405-325-7187.

a patient. Three different tissue types (skin, adipose tissue, and glandular tissue) were segmented and the postlumpectomy seroma was simulated inside the digital breast phantom. A treatment plan was made with three beam angles to deliver radiation dose to the seroma in breast to simulate SPBI. The three beam angles for 2D simulations were 17°, 90° and 159° (couch angles were 0 degrees) while the angles were 90 degrees (couch angles were 0°, 27°, 90°) in 3D simulation. A multi-step simulation platform capable of modelling XACT was developed. First, the dose distribution was converted to an initial pressure distribution. The propagation of this pressure disturbance in the form of induced acoustic waves was then modeled using the k-wave MATLAB toolbox. The waves were then detected by a hemispherical-shaped ultrasound transducer array (6320 transducer locations distributed on the surface of the breast). Finally, the time-varying pressure signals detected at each transducer location were used to reconstruct an image of the initial pressure distribution using a 3D time-reversal reconstruction algorithm. Finally, the reconstructed XACT images of the radiation beams were overlaid onto the structure breast CT.

Results: It was found that XACT was able to reconstruct the dose distribution of SPBI in 3D. In the reconstructed 3D volumetric dose distribution, the average doses in the GTV (Gross Target Volume) and PTV (Planning Target Volume) were 86.15% and 80.89%, respectively. When compared to the treatment plan, the XACT reconstructed dose distribution in the GTV and PTV had a RMSE (root mean square error) of 2.408 % and 2.299 % over all pixels. The 3D breast XACT imaging reconstruction with time-reversal reconstruction algorithm can be finished within several minutes.

Conclusions: This work explores the feasibility of using the novel imaging modality of XACT as an *in vivo* dosimeter for SPBI radiotherapy. It shows that XACT imaging can provide the x-ray beam location and dose information in deep tissue during the treatment in real time in 3D. This study lays the groundwork for a variety of future studies related to the use of XACT as a dosimeter at different cancer sites.

Keywords

3D dose monitoring; in real time; three-dimensional (3D) x-ray beam tracking; x-ray-induced acoustic computed tomography (XACT)

1. INTRODUCTION

In 2020, an estimated 276480 new cases of invasive breast cancer are expected to be diagnosed in women in the U.S.[1,2] Radiation therapy is traditionally utilized in stages I–III breast cancer as a local therapy after surgical management to improve disease-free survival and in some cases overall survival.[3] As a new technology, stereotactic body radiotherapy (SBRT) not only improves normal tissue sparing, but also delivers higher radiation dose to the tumor through several fractions.[4] In recent years, SBRT has been investigated to apply for early-stage breast cancer, that is, stereotactic partial breast irradiation (SPBI).[5-8] It is essential for SPBI to deliver accurate radiation dose to tumor; however, traditional radiotherapy workflow cannot meet this requirement.[5] In addition, the occurrence of lumpectomy shrinkage and radiation-induced breast swelling leads to large interfraction geometric uncertainties.[9,10] There also appear some unpredictable intrafraction geometric uncertainties because of the involuntary breathing movement.[11,12] Current treatment

planning for prone breast treatments requires large margins and therefore increased dose to normal breast tissue and adjacent critical organs to mitigate delivery uncertainties. Therefore, there is a great need for the development of high-resolution three-dimensional (3D) *in vivo* dosimetry techniques for real-time monitoring of the radiation dose in patients during SPBI.

X-ray acoustic computed tomography (XACT) is an emerging imaging modality that forms images by detecting acoustic waves induced via the x-ray-induced acoustic effect following a pulse of x-ray radiation.[13,14] X-ray acoustic computed tomography has been proposed as an *in vivo* dosimetry tool and has been investigated by several different groups.[15-19] It has been discovered that XACT signals are linearly proportional to x-ray dose deposition.[15] Initial studies applying XACT to linear accelerator (LINAC) photon beam dosimetry focused on the detection of the acoustic waves induced following the irradiation of metal blocks, due to the high Grüneisen coefficient of metals.[15] Later studies used XACT to image different shapes and sizes dose distributions in a homogeneous water tank.[16] The XACT images were obtained by keeping the immersion transducer stationary while the LINAC collimator was rotating. The acoustic signals were collected every 6° around the radiation field and images were then reconstructed. By comparing the XACT image profiles with the ion chamber measurement results, they verified there was a linear relationship between the XACT image intensity and the radiation dose.[16] Subsequent XACT characterization studies showed that the dose can decrease to 11.6 mGy to form XACT image with an acceptable SNR.[20] Recently, XACT with biological tissue phantoms as a sample has been demonstrated by Lei et al. on veal liver.[17] In their study, the authors employed conventional ultrasound imaging combined with XACT imaging. The beam intensity and its position relative to the fat tissue mass was clearly visible, and beam alignment could be monitored in addition to dose distribution, representing the first XACT deployment in a biological sample. These latest studies demonstrated the feasibility of using XACT as a viable dosimetry technique in a clinical radiotherapy environment. However, it currently takes tens of minutes to get a two-dimensional (2D) image with the current XACT imaging system, which renders real-time mapping of the dose during radiation therapy impossible.[15-17,21]

In this paper, we developed a simulation workflow to assess the ability of XACT to act as a 3D *in vivo* dosimetry tool for SPBI. First, the radiation dose distribution in the 3D digital breast phantom was converted to an initial pressure distribution using thermoacoustic equations. Acoustic propagation is then modeled throughout the media and detected by a hemispherical-shaped ultrasound transducer array using the k-wave MATLAB toolbox.[22] Finally, the time-varying pressure signals detected at each transducer location are then used to reconstruct an image of the initial pressure distribution using a 3D time-reversal reconstruction algorithm. Reconstructed XACT images of the radiation beams were overlaid onto the structure breast CT. We expect XACT imaging can be used to: (a) localize the radiation beam, and (b) estimate the radiation dose in real time during SPBI.

2. MATERIALS AND METHODS

2.A. Patient set-up and 3D breast XACT system configuration

Figure 1(a) shows the illustration of a breast XACT system configuration. The patient is made to lie on the board in a prone position, letting the irradiated breast hang down, which is placed in a hemispherical-shaped 3D ultrasound detectors array in Fig. 1(b). The relative position of the 2D slices to the breast volume is displayed in Fig. 1(c). A coupling medium (such as water) fills the array cavity to provide acoustic coupling. x-ray pulses generated by the accelerator irradiate the breast at three different incident angles. At the same time, ultrasound transducers around the breast collect x-ray-induced acoustic (XA) signals caused by thermoacoustic effects. The initial thermoacoustic pressure is proportional to x-ray energy absorbed, and therefore can be reconstructed in 3D [Fig. 1(d)], making it possible to monitor the position of the beams and map the deposited radiation dose *in vivo* during SPBI.

2.B. 3D breast digital phantom

A 3D breast digital phantom has been built from 3D breast CT images. The original CT image size is 512 × 512 × 487, corresponding to a breast volume with 15.7 cm (x) × 15.7 cm (y) × 9.3 cm (z). The breast images were segmented into three different tissue types: skin, adipose tissue, and glandular tissue according to an expectation–maximization (EM) algorithm slice by slice.[23] We then manually added irregularly shaped volume with a maximum diameter of 3.6 cm which represents the location of the seroma after the lumpectomy in Fig. 2. 3D breast digital phantom will be reconstructed from series of 2D slices.

2.C. Treatment planning for SPBI

To simplify the simulation process, a monogenetic x-ray beam (2 MeV) which was similar to the x-ray treatment beam from clinic LINAC machine (6 MV) was delivered in the breast from three different angles to achieve accumulated radiation dose on the location of the seroma. For the 2D simulation, we take slices along the x-axis of the breast volume and select the middle slice to simulate three different incident angle beams on the y-z plane. In this case, the 2D ultrasound detector is an arc-shaped matrix array and there are 380 ultrasound transducers evenly distributed around the breast slice. Correspondingly, the 3D simulation is implemented on the x-y plane; slices are selected along the z-axis of the breast volume and there are three beams simulated on the breast CT slices. A treatment plan was made with three beam angles to deliver radiation dose to the seroma in breast to simulate SPBI. For 2D simulations, the couch angle was 0° while the gantry angles were 17°, 90°, and 159°. For 3D simulations, the gantry angle was 90° while the couch angles were 0°, 27°, and 90°. The respective incident angles and beam widths of the three beams are shown in Table I.

2.D. Simulation workflow

We have built the simulation workflow on XACT imaging for *in vivo* dosimetry during SPBI. As is shown in Fig. 3, we first acquire and process a set of breast CT images, which includes segmenting the original image and embedding the seroma area into the breast.

Next, we design a sensor array for signal acquisition, including curved sensors for 2D simulation and bowl-sensor arrays for 3D simulation. Then we simulated the generation and propagation of x-ray-induced acoustic pressure in the breast with MATLAB toolbox k-Wave.[22] The center frequency and bandwidth of ultrasound transducer are 2.5 MHz and 100 %. A sampling frequency of 80 MHz was used to obtain the digital XA data.

The initial pressure reconstructed from the acoustic signal is converted into a relative dose distribution according to the proportional relationship between pressure and dose, and then image fusion is performed; the relative dose map is superimposed on the original breast CT image. Finally, the reconstructed relative dose distribution map is compared with the initial simulated dose distribution map to achieve a quantitative assessment of the patient's breast deposited dose during the radiotherapy simulation experiment.

The x-ray dose deposition and initial acoustic pressure distribution are calculated using the XA signals generation principles.[15,17,24,25] It has been found that there is a linear proportional relationship between the amplitude of acoustic pressure $\boldsymbol{p}(r)$ and the x-ray deposition dose D ($\boldsymbol{r}$),

$$\boldsymbol{p}(r) = \rho\Gamma(r)\,\mathrm{D}\,(\boldsymbol{r}), \tag{1}$$

where D ($\boldsymbol{r}$) is the radiation dose deposited at a given location $\boldsymbol{r}$. $\Gamma = \frac{\beta}{\kappa\rho C_{\mathbf{p}}}$ is the Grüneisen parameter which related to thermoelastic efficiency of the medium (Table II), where ρ is the mass density of the breast tissue, C_p is the specific heat capacity at constant volume, and $v_s = \sqrt{1 / \kappa\rho}$. The correlation between the initial pressure $p_0(r)$ and the local dose absorbed D(r) will reveal (a) the beam location and dose distribution according to information about the pressure field during irradiation, (b) the relative amount of dose delivered to the specific target where there may be differences due to undergoing diverse propagation mediums.

2.E. XACT image reconstruction

As mentioned in Section 2.D., x-ray-induced acoustic signals can be collected at each transducer around the breast, either by using an arc-shaped transducer array in 2D or by using a hemispherical-shaped ultrasound array in 3D. Then, all the detected x-ray-induced acoustic signals will be used to reconstruct XACT imaging with time-reversal reconstruction algorithm.[28] The principle of this reconstruction method is using the recorded time-varying pressure as a Dirichlet boundary condition enforced at the position of the detectors and then transmitted into the medium, which is the least sensitive reconstruction algorithm to any restrictions and more versatile as compared to the back-projection method.[29] The time reversal algorithm is a method of keeping spatial coordinates unchanged, inverting the signal propagation process in the time domain, and finally realizing the image reconstruction.[22,30] Compared with other imaging algorithms, the algorithm is not limited by the axiomatic derivation formula, has fewer constraints, is robust, and has fewer assumptions or initial conditions. It is suitable for image reconstruction of nonuniform sound velocity media and arbitrary scanning geometry. Moreover, it is not easily affected by image artifacts, and an ideal reconstruction effect can be obtained. It worth mentioning that the grid size used for reconstruction is the same as the previous forward model simulation.

3. RESULTS

3.A. XACT imaging for localizing the radiation beam in 2D

One of the unique advantages of XACT imaging is to localize the radiation beam inside the patient. In order to demonstrate this imaging capability, we simulated an x-ray beam irradiated into the breast from bottom to top which is displayed in Fig. 4. The breast slice and the curved sensor array are placed in a grid of 630 × 630. The spacing of the grid points in the x direction is 0.3063 mm, and the spacing in the y direction is 0.1912 mm. For the first XACT imaging [Fig. 4(a)], the x-ray beam was aligned with the position of the seroma area. To mimic the situation that the x-ray beam was off-target due to body motions or misplacement errors, the x-ray beam was shifted away from the target in second XACT imaging [Fig. 4(b)]. Three-line profiles at different positions were selected to quantify the relative dose intensity on XACT images at different depths. Therefore, we can visualize where the radiation beam is inside the patient and, we have the dose information of the patient. In future clinical practice, the radiation oncology team can adjust the location and direction of the beam quickly (or deactivate the beam) if there are any deviations being found from the treatment plan during the cancer treatment.

3.B. XACT imaging for 2D radiation dose map during SPBI

After simulating each segment, an XACT image of the dose distribution for a single fraction with three treatment angles was obtained by summing up each segment simulation during SPBI. Figure 5 shows the planned and reconstructed dose distributions for a single fraction in a representative slice in the center of the PTV. As shown in Figs. 5(a) and 5(b), we superimposed the initial relative dose distribution and the reconstructed radiation energy distribution onto the original breast CT slice. Then the range of GTV and PTV was delineated on the fusion image with color bars. In order to analyze the actual radiation delivered to the seroma area, we extracted the dose profile along the line at Y = 290 to obtain the initial dose deposition and the reconstructed XACT dose map for GTV and PTV, respectively. There are some numerical errors between the reconstructed dose and the initial dose deposition. It demonstrated that XACT imaging can be used for in-line radiation dose map during SPBI.

3.C. XACT imaging for localizing the radiation beam in 3D

While previous work has been limited to 2D, XACT is inherently 3D due to the spherical propagation of acoustic waves. A single projection x-ray exposure is sufficient to generate acoustic signals in 3D space because the x-ray generated acoustic waves are of a spherical nature and propagate in all directions from their point of generation.[24] We have simulated XACT imaging of the x-ray beam on top of breast CT imaging in 3D. Due to the limitation of computational cost, we first reduce the resolution of the 3D breast image and place it with the hemispherical sensor array in the grid of 330 × 330 × 330 for the 3D simulation, the grid spacing in the direction of x, y, z is 0.5228, 0.5528, 0.3267 mm respectively.

Figure 6 shows the planned [Fig. 6(a)] and reconstructed [Fig. 6(b)] XACT imaging dose distributions for a single fraction in a representative slice in 3D. Figure 6(c) shows the x-ray beams in three different planes. Furthermore, Figs. 6(d)-6(f) show the reconstruction XACT

imaging with different breast slices (slice 1, 2, 33, 34, 65, 66), respectively. All 3D volumetric images are displayed with the software Vaa3D (*3D Visualization-Assisted Analysis, Allen Institute, China*).

3.D. 3D XACT dose map on planning CT

One of the most promising aspects of using XACT for *in vivo* dosimetry is the potential of combining it with anatomical imaging information, for example, the planning CT. We have superimposed the reconstructed 3D XACT dose map on top of breast CT. Figure 7(a) reveals the dose-dependent 3D XACT images at different angles, in which three x-ray beams can be clearly visualized. With the 3D imaging capability, radiation dose map at any depth [Fig. 7(b)] in different planes can be viewed during the treatment. To quantitatively assess the accuracy of the reconstructed dose in XACT imaging, we calculated the root mean square error (RMSE).[31] The RMSE is defined as:

$$RMSE = \sqrt{\frac{\sum_{n=1}^{N}\left(X_{f,n} - X_{i,n}\right)^2}{N}},$$

where N is the number of pixels within the GTV or PTV for the dose distribution, $X_{f,n}$ is the nth pixel within GTV or PTV for the reconstructed dose distribution, and $X_{i,n}$ is the nth pixel within GTV or PTV for the initial or planned dose distribution. First, we calculated the RMSE values of all the breast slices in the range including GTV and PTV, which is 2.408% and 2.299%, respectively. Then we calculated the RMSE in the GTV and PTV for each breast layer.

The RMSE between the planned and XACT reconstructed dose distributions for all slices of the SPBI containing GTV and PTV are shown in Fig. 7(c). There are 48 layers used for calculating RMSE for GTV while there are 66 layers used for calculating RMSE for PTV. We can clearly see that although the number of layers of GTV and PTV are different. From the first layer to the last layer of the irradiated breast, the RMSE value gradually decreases. In the GTV range, the median and average of RMSEs are 2.343% and 2.465%, respectively. In the PTV range, the median and average RMSEs are 2.408% and 2.299%, respectively. Compared with the previous dose simulated by Monte Carlo,[32] our dose difference is larger, which is caused by the limitation of the time-reversal reconstruction algorithm. The RMSE values calculated in their Monte Carlo simulation were all lower than 1%, while our values were all above 1%, which can be improved in the future. Moreover, in the reconstructed 3D volumetric dose distribution, the average doses in the gross target volume (GTV) and planning target volume (PTV) ranges were 86.15% and 80.89%, respectively. Therefore, we believe XACT imaging could allow for the verification of radiation dose being delivered to the desired location in the patient in 3D with combined information from planning CT.

4. DISCUSSIONS

XACT is a promising technique for *in vivo* dosimetry during SPBI. It has many advantageous characteristics that make its implementation as a radiotherapy dosimeter attractive: (a) XACT is a real-time technique, meaning *in vivo* images can be obtained

during treatment to ensure the delivered dose distribution is as expected. (b) XACT is an absolute dosimetry technique if the thermal expansion coefficient, physical density, and Gruneisen coefficient are accurately determined, and the transducer and amplification system is well defined and calibrated. (c) XACT can provide the dose map in 3D. (d) Dose information from XACT imaging can be combined with anatomical information from planning CT.

Our simulation studies show that XACT is an emerging technique which has the potential to be an *in vivo* dosimeter. XACT can provide an effective way to validate the implementation of treatments in real time, because acoustic waves are induced and detected after a single-pulse radiation. There is no need to implant any invasive dosimeter and it does not depend on indirect exit dosimetry techniques.[33,34] Since most stereotactic treatments use some form of iMRT (intensity modulated radiotherapy), the capability of real-time dose measurement with XACT imaging would resolve the intensity changes in real time. The current simulation is based on the LiNAC machine which has been used for Accelerated Partial Breast irradiation. XACT imaging can also be applied to different radiotherapy machine, for example, CyberKnife treatments are nonisocentric, where beams can be directed from any desired angle.[6]

At present, when applying XACT to practical clinical *in vivo* dose measurements, the image resolution we can achieve is still a challenging problem. The LiNAC pulse duration in clinic is usually between 3 and 4 μs, the corresponding in-water spatial resolution is 4.4-5.9 mm.[33] More signal processing techniques, such as deconvolution, are necessary to address this problem in our future research. A recent experiment on XACT imaging demonstrated that high frequency ultrasound signals can be detected with a 2.5 MHz transducer because of the fast rising and falling edge of the x-ray pulses. An imaging resolution around 1.3 mm can be achieved during the experiment.[35]

Our current studies have displayed relative dose information with XACT images; however, it could be possible to use XACT for absolute dosimetry measurements provided the heat defect, physical density and Gruneisen coefficient are accurately known, and the transducer and amplification system is well calibrated and characterized.[18]

While previous work has been limited to 2D,[15,16,21,31] XACT is inherently 3D due to the spherical propagation of acoustic waves, and 3D images have been reconstructed with our 3D ultrasound array. In our simulation, 6320 sensor positions have been distributed on a 3D hemisphere. The physical radius of the 3D hemispherical transducer array is 7.2 cm, and each sensor has an area of 5.71 mm^2 to receive the acoustic signal. With the rapid development of 3D breast ultrasound imaging device, ultrasound array with thousands of elements has been fabricated recently.[36] Another advantage for XACT to be an *in vivo* dosimetry is its potential to be combined with anatomical ultrasound imaging. The B-mode ultrasound images and the radiation-induced signals can be obtained by the same transducer. This means that we can get the anatomical information and dose distribution at the same time. Based on these, the expected acoustic signals can be simulated according to patients' treatment plan prior to treatment delivering. Once the acoustic signals are found to be different from the planned expectation, the radiotherapy is immediately stopped. Making use

of the target tracking of ultrasound, it is practical to verify whether the dose is being delivered to the patient's intended location in real time. The ultrasound array may block part of the x-ray beam when it goes through the array, causing geometry nonuniformity of the irradiated x-ray intensity and overlaying a pattern on the breast XACT images. We can address this problem from both perspectives of software and hardware.[37] The lifetime of the ultrasound might be reduced because of receiving radiation during the cancer treatment. Concerns on skin-related toxicities because of coupling water might reduce the skin sparing effect of the MV x-rays will be also considered in the clinical translation of XACT imaging.

5. CONCLUSIONS

This study explored the feasibility of using XACT for *in vivo* dosimetry during SPBI radiotherapy has been conducted in this study via simulations. Based on breast CT images, a 3D breast volume was rendered with different tissue types. Numerical simulations illustrated the process of radiotherapy using two model x-ray beams to irradiate the seroma area in the breast phantom. After the x-ray-induced initial pressure distribution inside the breast being reconstructed via a time-reversal algorithm, the relative dose map can be obtained according to the proportional relationship between the initial pressure and the dose deposition. The final energy profile is superimposed on the original breast CT image to achieve real-time tracking of the beam position and relative dose monitoring. Results show that GTV and PTV for evaluating radiotherapy effects were adequately irradiated in the reconstructed dose distribution map. Furthermore, the RMSE values in the GTV and PTV were calculated. The proposed system configuration has great potential to be applied as a dosimeter for SPBI.

ACKNOWLEDGMENTS

This work was funded by the National Natural Science Foundation of China (nos. 61471226, 61741117 and 11747085), Natural Science Foundation of Shandong Province (nos. JQ201516, 2018GGX101018), and the Taishan Scholar Project of Shandong Province (no. tsqn20161023) to support the Yue Zheng's visit of Dr. Liangzhong Xinag's lab in The University of Oklahoma. This work was also partially supported by the National Institute of Health (R37CA240806), American Cancer Society (133697-RSG-19-110-01-CCE), and the Oklahoma Center for the Advancement of Science and Technology (HR19-131). The authors would like to acknowledge the support from Stephenson Cancer Center bridge fund, IBEST-OUHSC fund, and a grant from the Research Council of the University of Oklahoma Norman Campus as well. The authors would like to thank Elijah Robertson for proofreading the manuscript.

REFERENCES

1. DeSantis CE, Ma J, Gaudet MM, et al. Breast cancer statistics. CA Cancer J Clin. 2019;69:438–451. [PubMed: 31577379]
2. Statistics USBC. https://www.breastcancer.org/symptoms/understand_bc/statistics; 2019.
3. Jutzy JMS, Lemons JM, Luke JJ, Chmura SJ. The evolution of radiation therapy in metastatic breast cancer: from local therapy to systemic agent. Int J Breast Cancer. 2018;2018:4786819. [PubMed: 29862083]
4. Benedict SH, Yenice KM, Followill D, et al. Stereotactic body radiation therapy: the report of AAPM Task Group 101. Med Phys. 2010;37:4078–4101. [PubMed: 20879569]
5. Chiu TD, Parsons D, Zhang Y, et al. Prototype volumetric ultrasound tomography image guidance system for prone stereotactic partial breast irradiation: proof-of-concept. Phys Med Biol. 2018;63:055004. [PubMed: 29405123]

6. Obayomi-Davies O, Kole TP, Oppong B, et al. Stereotactic accelerated partial breast irradiation for early-stage breast cancer: rationale, feasibility, and early experience using the cyberknife radiosurgery delivery platform. Front Oncol. 2016;6:129. [PubMed: 27242967]
7. Rahimi A, Timmerman R. New techniques for irradiating early stage breast cancer: stereotactic partial breast irradiation. Semin Radiat Oncol. 2017;27:279–288. [PubMed: 28577835]
8. Snider JW 3rd, Mutaf Y, Nichols E, et al. Projected improvements in accelerated partial breast irradiation using a novel breast stereotactic radiotherapy device: a dosimetric analysis. Technol Cancer Res Treat. 2017;16:1031–1037. [PubMed: 28705082]
9. Michalski A, Atyeo J, Cox J, Rinks M. Inter- and intra-fraction motion during radiation therapy to the whole breast in the supine position: a systematic review. J Med Imaging Radiat Oncol. 2012;56:499–509. [PubMed: 23043567]
10. Jones S, Fitzgerald R, Owen R, Ramsay J. Quantifying intra- and inter-fractional motion in breast radiotherapy. J Med Radiat Sci. 2015;62:40–46. [PubMed: 26229666]
11. Yue NJ, Goyal S, Kim LH, Khan A, Haffty BG. Patterns of intrafractional motion and uncertainties of treatment setup reference systems in accelerated partial breast irradiation for right- and left-sided breast cancer. Pract Radiat Oncol. 2014;4:6–12. [PubMed: 24621417]
12. Jagsi R, Ben-David MA, Moran JM, et al. Unacceptable cosmesis in a protocol investigating intensity-modulated radiotherapy with active breathing control for accelerated partial-breast irradiation. Int J Radiat Oncol Biol Phys. 2010;76:71–78. [PubMed: 19409733]
13. Xiang L, Ahmad M, Carpenter C, et al. X-ray acoustic computed tomography: concept and design. Med Phys. 2013;40:522.
14. Xiang L, Ahmad M, Nikoozadeh A, Pratx G, Khuri-Yakub B, Xing L. X-ray acoustic computed tomography (xact): 100% sensitivity to x-ray absorption. Med Phys. 2014;41:448.
15. Xiang L, Han B, Carpenter C, Pratx G, Kuang Y, Xing L. X-ray acoustic computed tomography with pulsed x-ray beam from a medical linear accelerator. Med Phys. 2013;40:010701. [PubMed: 23298069]
16. Hickling S, Lei H, Hobson M, Leger P, Wang X, El Naqa I. Experimental evaluation of x-ray acoustic computed tomography for radiotherapy dosimetry applications. Med Phys. 2017;44:608–617. [PubMed: 28121381]
17. Lei H, Zhang W, Oraiqat I, et al. Toward in vivo dosimetry in external beam radiotherapy using x-ray acoustic computed tomography: A soft-tissue phantom study validation. Med Phys. 2018;45:4191–4200.
18. Forghani F, Mahl A, Patton TJ, et al. Simulation of x-ray induced acoustic imaging for absolute dosimetry: accuracy of image reconstruction methods. Med Phys. 2019;47:1280–1290.
19. Samant P, Chen Y, Wang S, et al. Towards in vivo dosimetry with x-ray acoustic computed tomography (XACT). Med Phys. 2019;46:E366.
20. Hickling S, Hobson M, El Naqa I. Characterization of x-ray acoustic computed tomography for applications in radiotherapy dosimetry. IEEE Trans Radiat Plasma. 2018;2:337–344.
21. Hickling S, Leger P, El Naqa I. On the detectability of acoustic waves induced following irradiation by a radiotherapy linear accelerator. IEEE Trans Ultrason Ferroelectr Freq Control. 2016;63:683–690. [PubMed: 26886983]
22. Treeby BE, Cox BT. k-Wave: MATLAB toolbox for the simulation and reconstruction of photoacoustic wave fields. J Biomed Opt. 2010;15:021314. [PubMed: 20459236]
23. Carson C, Belongie S, Greenspan H, Malik J. Blobworld: image segmentation using expectation-maximization and its application to image querying. IEEE Trans Pattern Anal. 2002;24:1026–1038.
24. Xiang L, Tang S, Ahmad M, Xing L. High resolution x-ray-induced acoustic tomography. Sci Rep. 2016;6:26118. [PubMed: 27189746]
25. Tang S, Nguyen DH, Zarafshani A, et al. X-ray-induced acoustic computed tomography with an ultrasound transducer ring-array. Appl Phys Lett. 2017;110:103504.
26. Seltzer S Tables of X-ray mass attenuation coefficients and mass energy-absorption coefficients. NISTIR-5632; 1996.
27. Hasgall PA, Di Gennaro F, Baumgartner C, et al. IT'IS Database for thermal and electromagnetic parameters of biological tissues; 2012.

28. Cox BT, Treeby BE. Artifact trapping during time reversal photoacoustic imaging for acoustically heterogeneous media. IEEE Trans Med Imaging. 2010;29:387–396. [PubMed: 19887310]
29. Hristova Y, Kuchment P, Nguyen L. Reconstruction and time reversal in thermoacoustic tomography in acoustically homogeneous and inhomogeneous media. Inverse Probl. 2008;24:055006.
30. Treeby BE, Zhang EZ, Cox BT. Photoacoustic tomography in absorbing acoustic media using time reversal. Inverse Probl. 2010;26:115003.
31. Hickling S Feasibility of x-ray acoustic computed tomography as a relative and in vivo dosimeter in radiotherapy application. McGill Universit; 2014.
32. Rodriguez M, Sempau J, Fogliata A, Cozzi L, Sauerwein W, Brualla L. A geometrical model for the Monte Carlo simulation of the TrueBeam linac. Phys Med Biol. 2015;60:N219–N229. [PubMed: 25984796]
33. Hickling S, Xiang L, Jones KC, et al. Ionizing radiation-induced acoustics for radiotherapy and diagnostic radiology applications. Med Phys. 2018;45:e707–e721. [PubMed: 29679491]
34. Sampaio DRTUJ, Antonio AO, Pavoni JF, Pavan TZ. X-ray acoustic imaging for external beam radiation therapy dosimetry using a comercial ultrasound scanner. IEEE Int Ultrason Symp (IUS). 2015;2015:1–4.
35. Lei H. Developments and Applications of Laser-Based and X-Ray-Based Biomedical Thermoacoustic Imaging Techniques. PhD dissertation; 2019.
36. Wiskin J, Malik B, Natesan R, et al. Full wave 3D inverse scattering transmission ultrasound tomography: breast and whole body imaging. IEEE Int Ultrason Symp (IUS). 2019;2019:951–958.
37. Tang S, Yang K, Chen Y, Xiang L. X-ray-induced acoustic computed tomography for 3D breast imaging: a simulation study. Med Phys. 2018;45:1662–1672. [PubMed: 29479717]

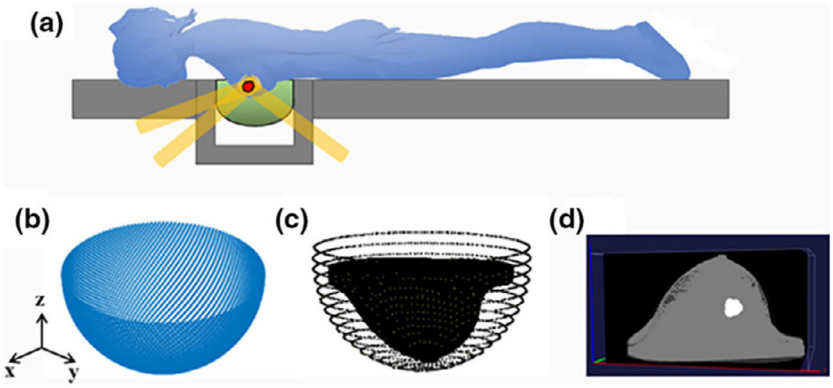

Fig. 1.

An illustration of the three-dimensional (3D) breast x-ray-induced acoustic computed tomography system configuration. (a) The patient is made to lie on the couch, letting the breast surrounded by the ultrasound arrays. Three cylindrical x-ray beams irradiate the seroma area in the breast with different angles. (b) 3D hemispherical-shaped ultrasound arrays. (c) The relative position of the two-dimensional slices to the breast volume. (d) The 3D view of breast volume. The bright volume in the breast represents the location of seroma area.

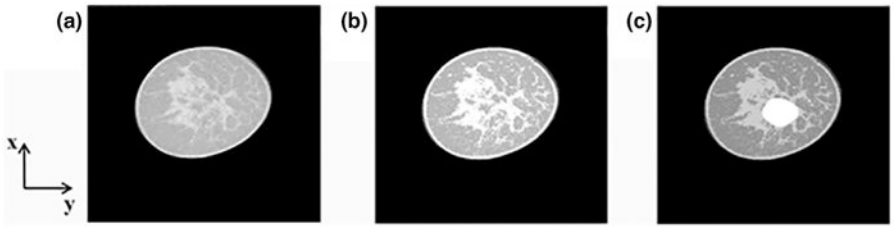

Fig. 2.

Breast digital phantom rendered from breast computed tomography (CT) slices. (a) A typical breast CT slice along the x-y plane. (b) The segmentation of (a) with three tissue types: the skin, adipose tissue, and glandular tissue. (c) The location of the seroma after the lumpectomy has been simulated in a segmented breast image.

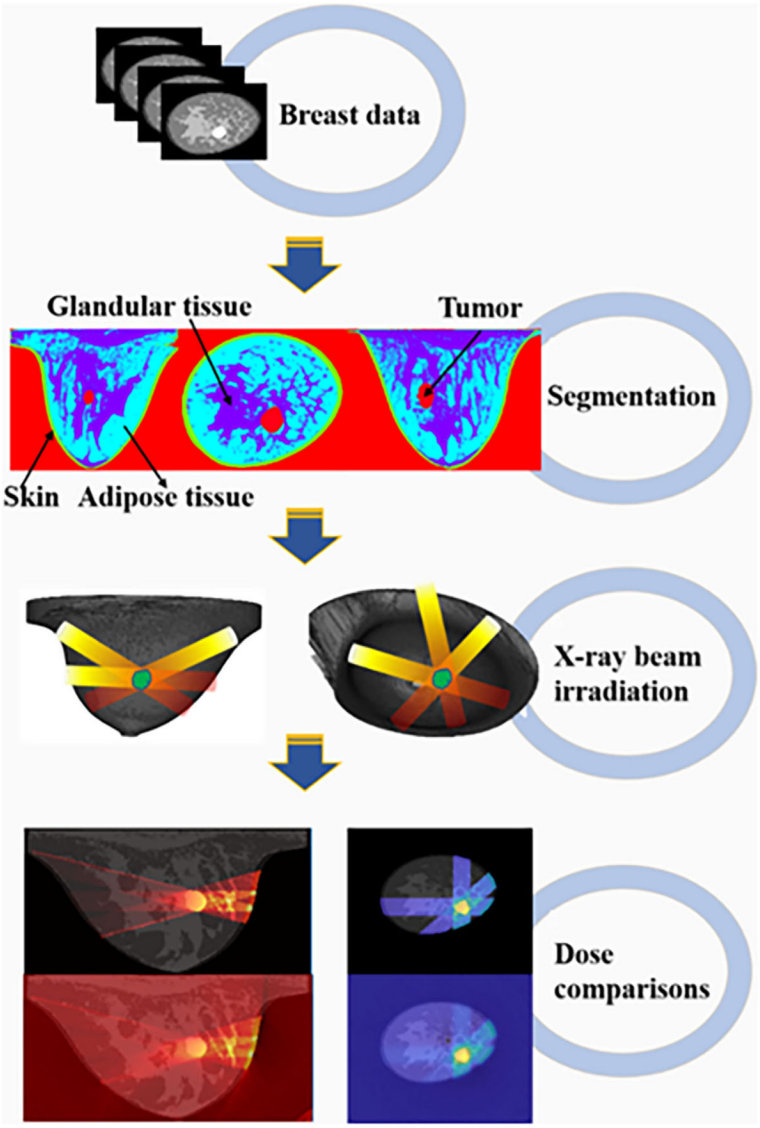

Fig. 3.
Flow chart of x-ray-induced acoustic computed tomography imaging for radiation dose verification in SPBI.

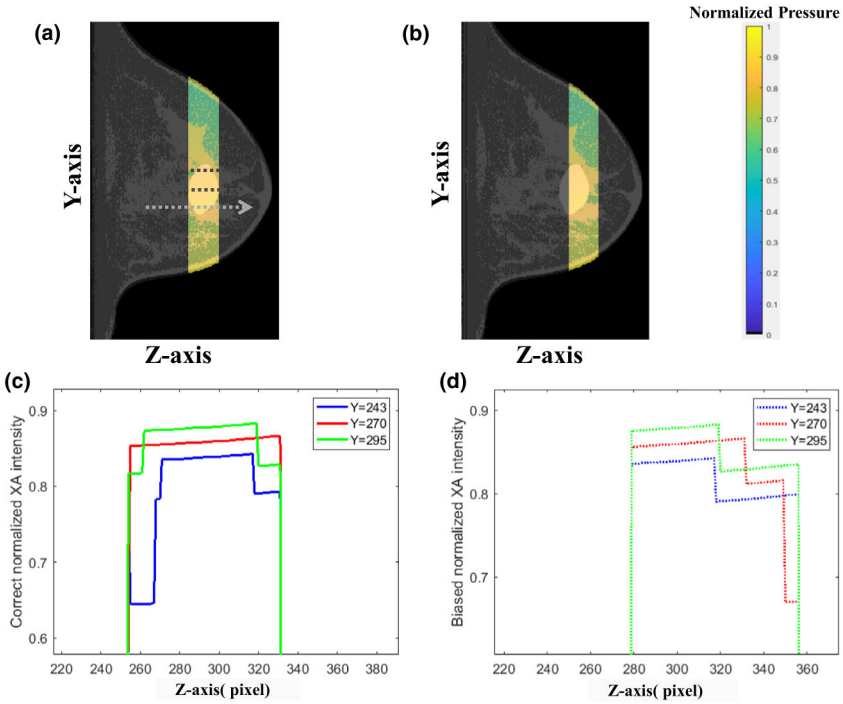

Fig. 4.

Verification of x-ray-induced acoustic computed tomography (XACT) imaging for radiation beam localization during SPBI. A two-dimensional breast slide was used to simulate radiotherapy with an x-ray beam irradiated from the bottom to the top. (a) x-ray beam was aligned with the position of the targeted treatment area. (b) x-ray beam was off-target due to body motions or misplacement errors. (c) A dose profile has been extracted from XACT image [Fig. 4(a)] at Y = 243, Y = 270 and Y = 290, respectively. (d) A dose profile has been extracted from XACT image [Fig. 4(b)] at Y = 243, Y = 270 and Y = 290, respectively.

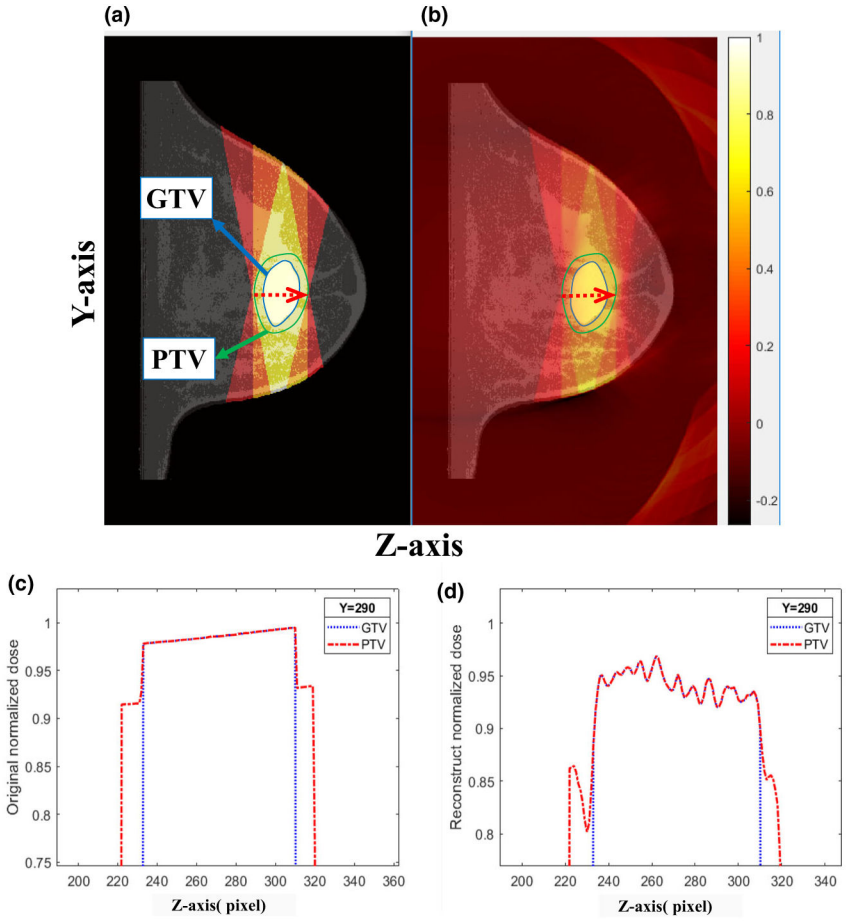

Fig. 5.

Planned (a) and x-ray-induced acoustic computed tomography (XACT) reconstructed (b) dose distributions for a single fraction in a representative slice in the center of the PTV for the SPBI case. A dose profile has been extracted from planned dose distribution (a) and XACT image (b) at Y = 290.

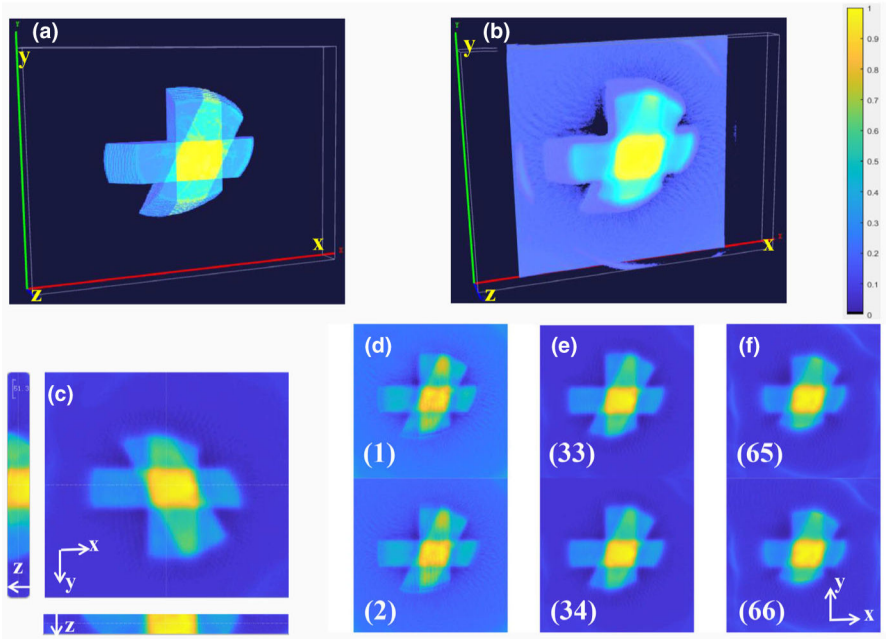

Fig. 6.

Planned (a) and x-ray-induced acoustic computed tomography (XACT) reconstructed (b) dose distributions in three-dimensional for a single fraction for a SPBI case. (c) shows the different sections of the XACT reconstructed dose distribution in three planes (X-Y plane, X-Z plane, Y-Z plane). (d)-(f) show the reconstruction XACT imaging with different breast slices (slice 1, 2, 33, 34, 65, 66), respectively.

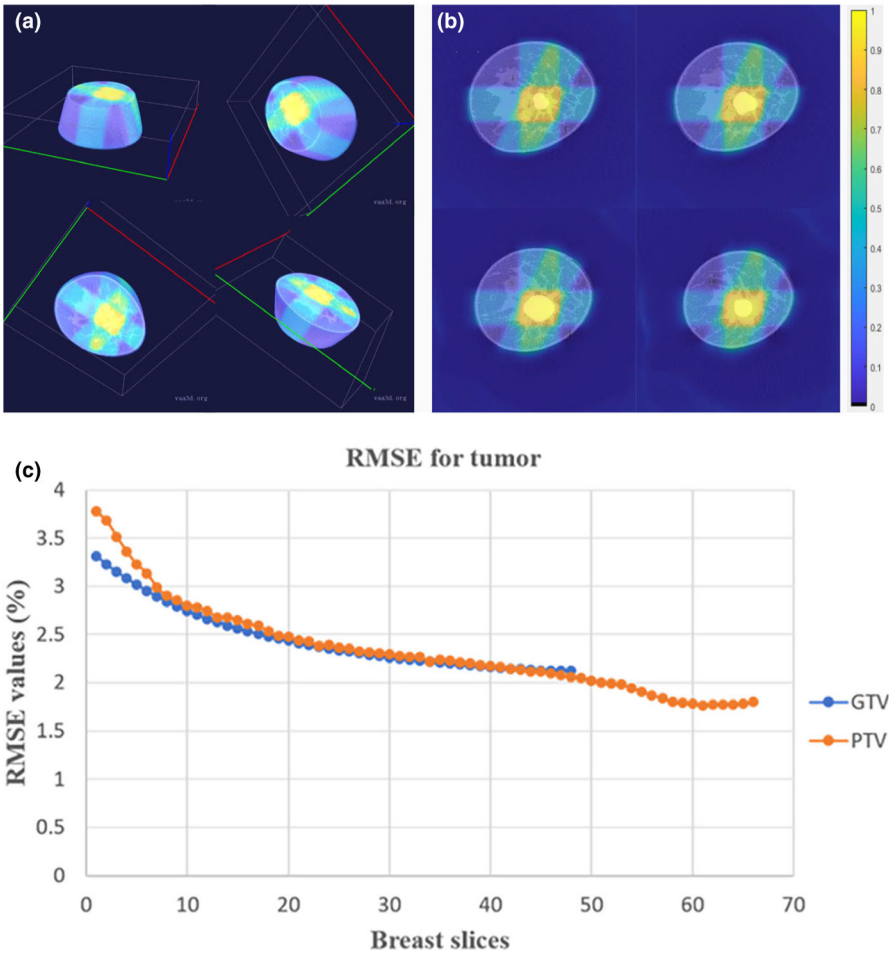

Fig. 7.

Three-dimensional dose map with combined x-ray-induced acoustic computed tomography (XACT) imaging and planning computed tomography (CT). (a) three-dimensional dose map with XACT images overlap on the breast CT image viewed by 4 different angles. (b) dose map with combined XACT imaging and breast CT at different sections. (c) RMSE values of the GTV and the PTV for all slices.

Table I.

The specification of beams.

Beam parameters	X-ray effective energy (MeV)	Gantry angle (couch angle)			Width (cm)		
		1	2	3	1	2	3
2D	2	17 (0)	90 (0)	159 (0)	2.1	2.1	2.8
3D	2	90 (0)	90 (27)	90 (90)	2.6	3.0	3.1

Table II.

Thermoelastic parameters for the breast tissues.[26,27]

Tissue	ρ (kg/m^3)	v_s (m/s)	β (×10^{-4}/K)	C_P(J/kg · K)	μ_a (cm^2/g)	μ_{en} (cm^2/g)	Grüneisen parameter
Skin	1100	1537	3.0	3390.5	0.02601	0.04925	0.209
Adipose tissue	900	1450	2.08	2348.3	0.0261	0.0494	0.1862
Glandular tissue	1020	1510	2.08	2348.3	0.02592	0.0491	0.202
Seroma	1050	1700	3.0	3017	0.0290	0.04896	0.2874